This article was downloaded by:
On: *25 January 2011*
Access details: *Access Details: Free Access*
Publisher *Taylor & Francis*
Informa Ltd Registered in England and Wales Registered Number: 1072954 Registered office: Mortimer House, 37-41 Mortimer Street, London W1T 3JH, UK

Liquid Crystals
Publication details, including instructions for authors and subscription information:
http://www.informaworld.com/smpp/title~content=t713926090

An improved equivalent circuit model and the dependence of hysteresis inversion frequency on typical parameters of V-shaped switching SSFLC cells for both bookshelf and chevron structures

M. Y. Wang[a]; W. Pan[a]; B. Luo[a]; W. L. Zhang[a]; X. H. Zou[a]
[a] Library of Optical Communications, School of Information Science & Technology, Southwest Jiaotong University, Chengdu, Sichuan, P. R. China

To cite this Article Wang, M. Y. , Pan, W. , Luo, B. , Zhang, W. L. and Zou, X. H.(2008) 'An improved equivalent circuit model and the dependence of hysteresis inversion frequency on typical parameters of V-shaped switching SSFLC cells for both bookshelf and chevron structures', Liquid Crystals, 35: 3, 373 — 379
To link to this Article: DOI: 10.1080/02678290801902549
URL: http://dx.doi.org/10.1080/02678290801902549

PLEASE SCROLL DOWN FOR ARTICLE

Full terms and conditions of use: http://www.informaworld.com/terms-and-conditions-of-access.pdf

This article may be used for research, teaching and private study purposes. Any substantial or systematic reproduction, re-distribution, re-selling, loan or sub-licensing, systematic supply or distribution in any form to anyone is expressly forbidden.

The publisher does not give any warranty express or implied or make any representation that the contents will be complete or accurate or up to date. The accuracy of any instructions, formulae and drug doses should be independently verified with primary sources. The publisher shall not be liable for any loss, actions, claims, proceedings, demand or costs or damages whatsoever or howsoever caused arising directly or indirectly in connection with or arising out of the use of this material.

Liquid Crystals,
Vol. 35, No. 3, March 2008, 373–379

Taylor & Francis
Taylor & Francis Group

An improved equivalent circuit model and the dependence of hysteresis inversion frequency on typical parameters of V-shaped switching SSFLC cells for both bookshelf and chevron structures

M. Y. Wang*, W. Pan, B. Luo, W. L. Zhang and X. H. Zou

Library of Optical Communications, School of Information Science & Technology, Southwest Jiaotong University, Chengdu, Sichuan, P. R. China

(Received 4 November 2007; in final form 8 January 2008)

An improved equivalent circuit model able to be applied to conventional circuit simulators is presented for optical response prediction and drive circuit design of V-shaped surface-stabilised ferroelectric liquid crystal (SSFLC) cells. The model is derived from Moore and Travis' original model. Moreover, the impedance divider induced by the multilayer structure of the liquid-crystal cells is taken into account, and both polar and non-polar surface anchoring energy are considered to make the model more preferable. The model is then utilised to investigate the thresholdless switching characteristics for both bookshelf and chevron structures. With the circuit model: (1) the genuine V-shaped switching occurs only at the hysteresis inversion frequency f_i, and below (above) f_i an anomalous (normal) hysteresis is observed; (2) the genuine V-shaped switching is only observed when the transmission is plotted as a function of the total applied voltage; (3) f_i increases with increasing conductivity of liquid-crystal layer (G_{LC}) and the amplitude of applied voltage, and the function of $f_i\left(G_{LC}^{1/2}\right)$ is almost linear; (4) For small spontaneous polarisation p_s, f_i grows as p_s increases, however, on further increasing p_s, f_i reaches its maxima and then decreases (5) the V-shaped switching can be observed in both bookshelf and chevron structures, however, f_i is higher for the chevron structure. Results obtained from the circuit model compare favourably with the reported experimental and numerical results.

Keywords: surface-stabilised ferroelectric liquid crystal (SSFLC); V-shaped switching; hysteresis inversion frequency; chevron structure; equivalent circuit model

Downloaded At: 15:19 25 January 2011

1. Introduction

Ever since surface-stabilised ferroelectric liquid crystal (SSFLC) was first introduced by Clark and Lagerwall in 1980 (*1*), a large number of investigations have been performed (*2, 3*). Recently, thresholdless, hysteresis-free, V-shaped, electro-optical switching was discovered in the thin plane-parallel aligned cell of SSFLCs. V-shaped switching has attracted considerable attention due to its advantageous possibility of an analog gray scale. The chevron structure of the smectic layers is a well known characteristic of most SSFLC cells. General opinion has been that V-shaped switching is hardly compatible with chevron structures but, recently, it has been proposed that V-shaped switching exists also in SSFLC cells with chevron geometry (*4, 5*). The switching mechanism of V-shaped switching is still under discussion (*6–10*). Recently, the idea that V-shaped switching is an apparent rather than a real phenomenon of SSFLC cells has been put forward by Blinov et al. (*11–15*). The authors also proposed an equivalent circuit to describe the voltage divider constructed by the ferroelectric liquid-crystal (FLC) layer, alignment layer and the drive circuit. Due to this, even the optical transmittance shows a hysteresis at f_i when it is plotted as a function of the voltage on the FLC layer and not as a function of the total voltage. On the basis of the proposed circuit, a drive circuit for a fast-response display panel has been developed by Shwu-Yun et al. (*16, 17*).

The equivalent circuit proposed by Blinov et al. is solved by a numerical algorithm (*10, 15*). Moreover, performances of V-shaped switching are usually predicted by a numerical algorithm which might be written in Matlab, C++ or such like. However, since the voltage divider plays an important role in V-shaped switching, an equivalent circuit able to be applied to conventional circuit simulators, e.g. PSpice, is a promising alternative. An equivalent circuit is the natural model to describe and design the voltage divider, especially when the drive circuit and the drive voltage have comparatively complicated forms. Furthermore, the great majority of transistor-based components are now defined by libraries written in PSpice or such like, so it is expedient to stretch the circuit model for a single FLC cell into various FLC-based photoelectric devices. Thus the motivation of this paper is to consolidate the proposal of an equivalent circuit by Blinov et al. and to develop an improved equivalent circuit model which can be used in

*Corresponding author. Email: yaoyao_0526@163.com, yaoyao_0526@hotmail.com

ISSN 0267-8292 print/ISSN 1366-5855 online
© 2008 Taylor & Francis
DOI: 10.1080/02678290801902549
http://www.informaworld.com

optical response prediction and drive circuit optimisation for V-shaped switching SSFLC cells.

In this paper, we introduce Moore and Travis' equivalent circuit model (*18*) and apply it to the SSFLC cell. This model defines the rotation of FLC director as the charging voltage on a capacitor. This model has been investigated further in the $\tau - V_{\min}$ addressing model (*19*), binary phase modulation (*20*), the optically addressed spatial light modulator (*21*) and CMOS backplane (*22*). However, this model has failed to predict the performance of V-shaped switching since the voltage divider is not calculated and the restoring torque is generated from straight line sections. In the improved model, the voltage divider is considered, and both polar and non-polar surface-anchoring energy are included. First, we demonstrate the validity of the improved circuit model with the valuable model proposed by Blinov et al. Second, we adopt and generalise this model to study the variation of inversion frequency with three of the most important parameters in V-shaped switching (the conductivity of the liquid-crystal layer, spontaneous polarisation and the amplitude of applied voltage) for both bookshelf and chevron structures.

Downloaded At: 15:19 25 January 2011

2. Physics, dynamic equations and model establishment

2.1. *The chevron structure and the dynamic equations*

Chevron formation in smectic samples is a result of the layers anchoring normal or nearly normal to the bounding plates and subsequent layer contraction in the absence of dislocations. The generalised representation of SSFLC with a chevron structure is shown in Figure 1 (*23*), in which the director has the

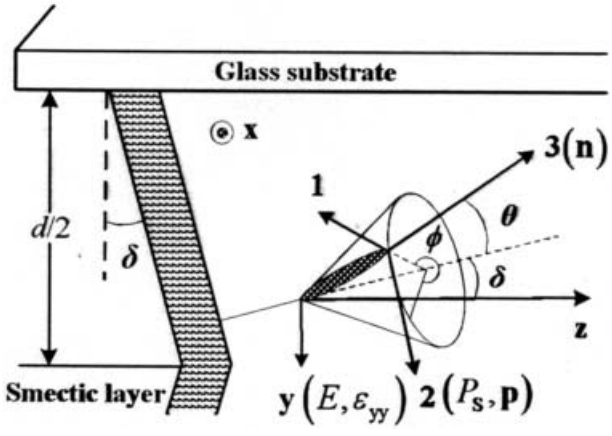

Figure 1. Generalised representation of FLC with a chevron structure. This figure shows the top part of the cell (*23*).

frame of reference in the director (***1***, ***2***, ***3***) and laboratory (***x***, ***y***, ***z***). The ***3*** direction is parallel to the director ***n***, the ***2*** direction normal to the director and to the tilted plane, and the ***1*** direction normal to these. ***p*** is the unit spontaneous polarisation vector and in the direction of ***2***-axis. The electric field of liquid-crystal layer is E, along the ***y***–axis. θ is the cone angle, δ is the chevron tilt angle, ϕ is the azimuth angle and d is the thickness of the FLC layer.

Generally speaking, the total free energy density f in an electric field E mainly depends on three different terms, the ferroelectric energy, the dielectric energy and the surface anchoring energy (*24*). The curvature elastic energy is neglected since the circuit model is based on the assumption that director and polarisation fields are spatially homogeneous. The free energy density f is given as

$$f = P_S E(\boldsymbol{p}\cdot\boldsymbol{y}) + \frac{W_{\text{anch}}}{d} \tag{1}$$

where P_S is spontaneous polarisation, E is the electric field of the liquid-crystal layer, W_{anch} is the strength of surface-anchoring energy. Here the dielectric energy is cancelled since it is not essential in this paper. Phenomenologically, the value of W_{anch} is expressed in terms of the scalar products and as follows (*25*):

$$W_{\text{anch}} = \sum_{v=\pm 1}\left[\frac{W_v}{2}(\boldsymbol{n}\cdot\boldsymbol{y})^2 + v W_v^{(P)}(\boldsymbol{p}\cdot\boldsymbol{y})\right]_{y=vd/2} \tag{2}$$

where W_1 (W_{-1}) is the strength of non-polar anchoring at the upper (lower) substrate, $W_1^{(P)}$ ($W_{-1}^{(P)}$) is the polar anchoring strength at the upper and lower substrate, respectively. It is seen form Equations (1) and (2) that in order to calculate the free energy f, the components of ***n*** and ***p*** along the ***y***-axis are required. These can be calculated from the transformation of the director axes frame to the laboratory axes frame. First, the coordinate is rotated by cone angle θ around the ***2***-axis.

This is followed by a rotation of ϕ around the 3-axis. This, in turn, is followed by a rotation of δ around the 1-axis. These successive rotations may be expressed as rotation matrices $\boldsymbol{R}_\theta$, $\boldsymbol{R}_\varphi$ and $\boldsymbol{R}_\delta$, and the FLC properties determined in the laboratory reference frame may be related to the director reference frame using the rotation $\boldsymbol{R}=(\boldsymbol{R}_\delta)(\boldsymbol{R}_\varphi)(\boldsymbol{R}_\theta)$. $\boldsymbol{R}$ is expressed as follows:

$$\boldsymbol{R} = \begin{bmatrix} \cos\phi\cos\theta & -\sin\phi & \cos\phi\sin\theta \\ \cos\delta\cos\theta\sin\phi+\sin\delta\sin\theta & \cos\delta\cos\phi & \cos\delta\sin\phi\sin\theta-\sin\delta\cos\theta \\ \sin\delta\sin\theta\sin\phi-\cos\delta\sin\theta & \sin\delta\cos\phi & \sin\delta\sin\phi\sin\theta+\cos\delta\cos\theta \end{bmatrix}. \tag{3}$$

The director in the laboratory frame of reference $(n_x, n_y, n_z)^T$ is related to the director in the director frame $(n_1, n_2, n_3)^T$ by

$$\begin{bmatrix} n_x \\ n_y \\ n_z \end{bmatrix} = \boldsymbol{R} \begin{bmatrix} n_1 \\ n_2 \\ n_3 \end{bmatrix} = \boldsymbol{R} \begin{bmatrix} 0 \\ 0 \\ 1 \end{bmatrix} = \begin{bmatrix} \cos\phi \sin\theta \\ \cos\delta \sin\phi \sin\theta - \sin\delta \cos\theta \\ \sin\delta \sin\phi \sin\theta + \cos\delta \cos\theta \end{bmatrix}. \quad (4)$$

Then the value of $(\boldsymbol{n}\cdot\boldsymbol{y})$ is $\cos\delta \sin\phi \sin\theta - \sin\delta \cos\theta$. Similarly, $(p_x, p_y, p_z)^T$ is related to $(p_1, p_2, p_3)^T$ by

$$\begin{bmatrix} p_x \\ p_y \\ p_z \end{bmatrix} = \boldsymbol{R} \begin{bmatrix} p_1 \\ p_2 \\ p_3 \end{bmatrix} = \boldsymbol{R} \begin{bmatrix} 0 \\ 1 \\ 0 \end{bmatrix} = \begin{bmatrix} -\sin\phi \\ \cos\delta \cos\phi \\ \sin\delta \cos\phi \end{bmatrix} \quad (5)$$

and the value of $(\boldsymbol{p}\cdot\boldsymbol{y})$ is $\cos\delta \cos\phi$. Combining Equations (1), (2), (4) and (5), the anchoring energy f is given by

$$f = P_S E \cos\delta \cos\phi + \frac{W}{2d}(\cos\delta \sin\phi - \sin\delta \cos\theta/\sin\theta)^2 - \frac{W_P}{d}\cos\delta \cos\phi \quad (6)$$

where $W=(W_1+W_{-1})\sin^2\theta$ is the strength of non-polar anchoring and $W_p = W_{-1}^{(p)} - W_1^{(p)}$ is the strength of polar anchoring, respectively. Then from the equation of motion, the time dependent behaviour of the director is as follows:

$$\gamma \frac{d\phi}{dt} = P_S E \cos\delta \sin\phi - \left[\frac{W}{d\sin\theta}(\cos\delta \sin\theta \sin\phi - \sin\delta \cos\theta) \cos\delta \cos\phi - \frac{W_p}{d}\cos\delta \sin\phi\right] \quad (7)$$

where γ is the rotational viscosity and t is time scale. Equation (7) is universally called the torque balance equation and its three parts from left to right are viscosity torque, ferroelectric torque and surface-anchoring torque, respectively. It is noted that in the equation, the electric field E is derived from $E=V_{LC}/d$, but not from $E=V_{IN}/d$. So, before dealing with the torque balance Equation (7), the voltage drop in the FLC layer V_{LC} is needed. At this stage the voltage divider, which might consist of the FLC layer, alignment layer and the drive circuit should be taken into account.

2.2. *The equivalent circuit model for V-shaped FLC cells*

Figure 2 shows the improved equivalent circuit model for the V-shaped switching SSFLC cells. The model is shown as three parts: as port electric characteristics of the cell, as reproducing physics and dynamic equations of a single cell, and as optical output, respectively.

In the simulation, triangular pulses are applied to drive the liquid-crystal device. C_P and R_P are the equivalent capacitor and resistor for alignment layers, similarly C_{LC} and R_{LC} are the equivalent capacitor and resistor for the FLC layer. Various drive circuits could be conveniently inserted into the model between ports 2 and 0. It can be seen from the model that the voltage drop on the FLC layer is $V(3,0)$; this is closely related to the voltage divider which is composed of the drive circuit, alignment layer and liquid-crystal layer. Thus the form of the voltage drop on the FLC layer can be very different from the form of the voltage drop on the total device. The differences no doubt affect the form of the field-induced optical transmission curve and a robust design should take this into account. For reproducing the physics and dynamic equations, the model used an integral capacitor C_{OUT} which is derived from Moore and Travis' PSpice equivalent circuit (*18*), with the voltage dropping on C_{OUT} (V_{COUT}) the

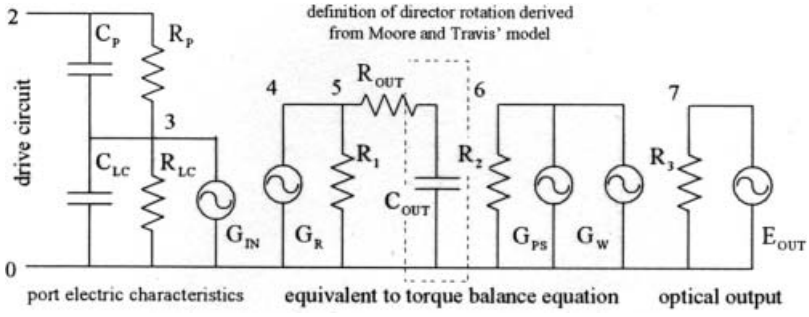

Figure 2. The improved equivalent circuit model for the V-shaped switching SSFLC cells.

Downloaded At: 15:19 25 January 2011

azimuth angle ϕ of FLC directors is represented. The three current sources G_R, G_{PS} and G_W are controlled by V_{COUT} and are equivalent to viscosity torque, ferroelectric torque and surface-anchoring torque, respectively. Thus the torque balance equation which describes the rotation mechanism of directors as a function of time, the voltage drop in the FLC layer and the parameters of the liquid crystal are consolidated in the circuit model. Finally, from the equivalent circuit, normalised light intensity is given by a voltage source E_{out} with which optical performances are measured in section 3.

3. Simulation results and discussion

The simulation parameters spontaneous polarisation $P_S=130\,\mathrm{nC\,cm^{-2}}$, rotational viscosity $\gamma=400\,\mathrm{mPa\cdot s}$, cone angle $\theta=35^\circ$, area $A=1.3\,\mathrm{cm^2}$, thickness of FLC layer $d=1.4\,\mu\mathrm{m}$ and two alignment layers each of thickness $d_P=40\,\mathrm{nm}$. With the dielectric constant $\varepsilon_P=3.8$ and the specific resistance $\rho_P=10^{14}\,\Omega\cdot\mathrm{cm}$, the capacitance of alignment layer is $C_P=\varepsilon_P A/4\pi k(2d_P)\approx 55\,\mathrm{nF}$ and the resistance is $R_p=\rho_p(2d_p)/A\approx 615\,\mathrm{M}\Omega$. Parameters mentioned above are directly derived from the experimental reports and the FLC mixture is PBH-13 (*11, 16, 26*). Other parameters are typical in FLCs: strength of non-polar anchoring $W=2\times10^{-4}\,\mathrm{J\,cm^{-2}}$ (*25*) and chevron tilt angle $\delta\approx 0.9\theta$ (*27*). The capacitance of FLC layer C_{LC} decreases as voltage increases, and with the voltage implemented in this study (higher than 1 V) C_{LC} can be negligible compared to C_p (*16*). The strength of polar anchoring W_p is set to be zero, so that it is not brought into play in this study.

3.1. *The hysteresis inversion frequency*

The switching mechanism of V-shaped switching is still under discussion; Blinov et al. propose that V-shaped switching of SSFLC cells is an apparent phenomenon rather than a real effect (*11*). We would like to repeat their viewpoint that firstly, V-shaped switching is observed only at one characteristic frequency f_i. Secondly, switching is accompanied by an inversion of the electro-optical hysteresis direction from the normal to the abnormal one. And finally, optical transmittance even shows a hysteresis at f_i when it is plotted as a function of the voltage on the FLC layer and not as a function of the total applied voltage. In Figures 3–5, we show that simulation results from the circuit model are in good agreement with the above results. Figure 3 illustrates a change in the hysteresis direction with $R_{LC}=10\,\mathrm{M}\Omega$. The optical transmittance of the cell induced by a triangular voltage form of amplitude

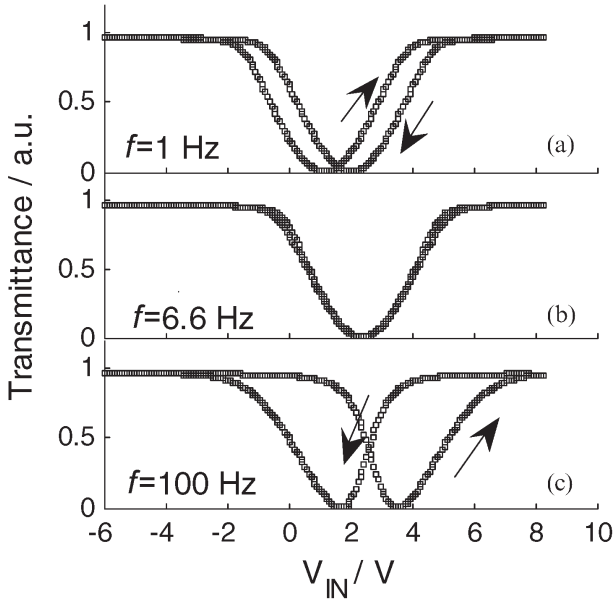

Figure 3. Transmittance controlled by a triangular voltage form of amplitude ± 8.3 V at different frequencies (from top to bottom): $f=1$ Hz, 6.6 Hz and 100 Hz.

± 8.3 V shows typical V-shaped electro-optical behavior at a frequency of 6.6 Hz, see in Figure 3 (b). Below and above this frequency an anomalous and normal hysteresis is observed for 1 Hz and 100 Hz, see Figures 3 (a) and 3 (c), respectively, and the arrows show the routes of the transmittance variation.

The voltage difference between two transmission minima of the W-letter (seen in Figures 3 (a) and 3 (c)) is defined as the coercive voltage V_C for FLC switching. The genuine V-shaped switching corresponds to $V_C=0$, seen in Figure 3 (b). The frequency dependence of V_C with different resistors of FLC layer is shown in Figure 4. The zero line separates the

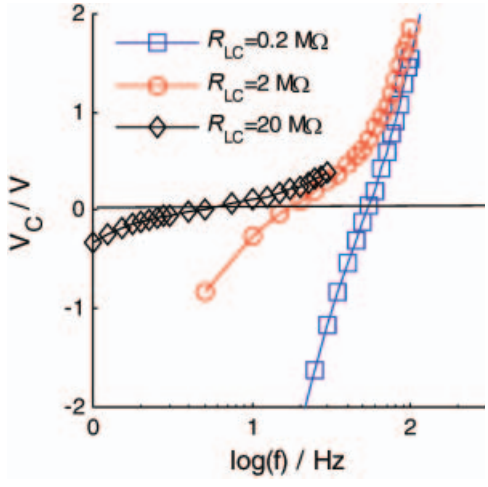

Figure 4. Coercive voltage, V_C, as a function of frequency with different R_{LC} of 0.2 MΩ, 2 MΩ and 20 MΩ, respectively.

Downloaded At: 15:19 25 January 2011

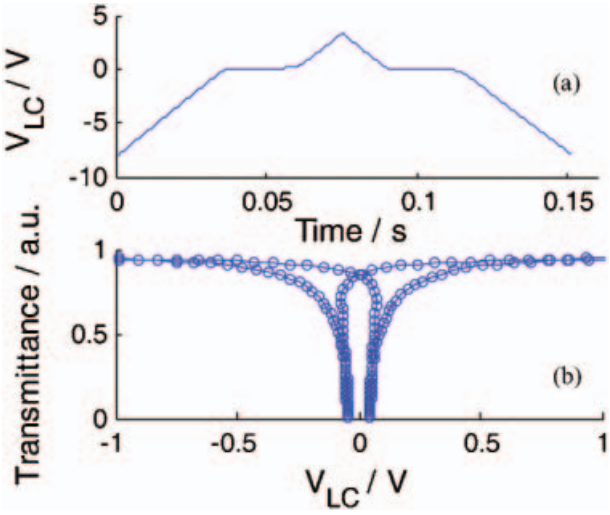

Figure 5. (a) The form of voltage on FLC layer, V_{LC}, the parameters are the same as in Figure 3 b (b) same transmittance of Figure 3 b replotted as a function of V_{LC}.

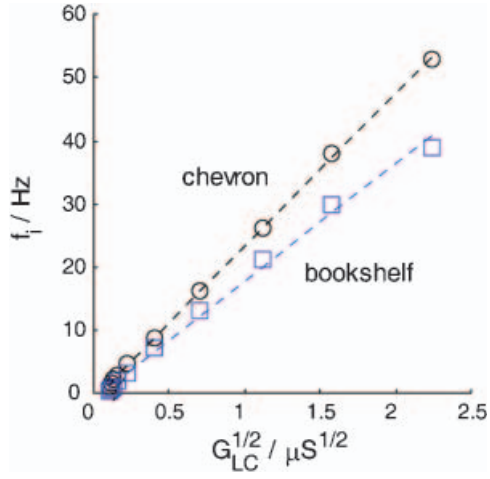

Figure 6. Comparison between the chevron and bookshelf structures of the dependence of the hysteresis inversion frequency on the square root of conductivity (other parameters are the same).

areas of the anomalous (below) and normal (above) hysteresis. It is seen that the coercive voltage is frequency-dependent and the genuine thresholdless switching is observed at only one frequency f_i which is universally called hysteresis inversion frequency.

With the same parameters of Figure 3 (b), the form of voltage dropping on FLC layer, V_{LC}, is given in Figure 5 (a). It is seen that the form of the curve of V_{LC} is distinctly different from the form of triangular pulses of the total applied voltage. The same optical transmittance is then replotted as a different coordinate, namely as a function of V_{LC}, see Figure 5 (b): the genuine V shape is diminished and a hysteresis typical for conventional FLC's is clearly seen in the curve.

From Figures 3–5, it is seen that simulation results from the circuit model are in good agreement with the laws given by the model of Blinov et al. (*11*). In fact, we also tried a set of values for many parameters, such as spontaneous polarisation, resistor of FLC layer, amplitude of the total voltage, chevron tilt angle and so on, and all the simulations show similar results as shown in Figures 3–5. The frequency f_i is very characteristic and important for understanding the V-shaped, hysteresis-free switching of FLCs. In the following sections, the circuit model is utilised to investigate the variation of f_i with different conductivities of liquid-crystal layers, amplitudes of applied voltage and the spontaneous polarisation for both bookshelf and chevron structures.

3.2. f_i *dependence on conductivity of liquid-crystal layer*

The dependence of the hysteresis inversion frequency f_i on the square root of conductivity of the FLC layer for both bookshelf and chevron structures are shown in Figure 6, in which the symbols ' ○ ' and '□' are directly derived from the circuit model and the dotted curves are fitted to the data. In the figure, the abscissa is selected in order to check a prediction of the simple analytical theory developed by Pikin (*11*). Indeed, the functions $f_i\left(G_{LC}^{1/2}\right)$ ($G_{LC}=1/R_{LC}$) are almost linear for both structures, as predicted. The same theory correctly describes the $f_i(C_P)$ dependence. Also, the same result (i.e. $f_i\left(G_{LC}^{1/2}\right)$ is almost linear) is given by Blinov *et al.* (*4*). From the figure it is also seen that f_i is increases with increasing conductivity from 0.17 Hz to 39 Hz for the bookshelf structure (see the lower curve) and rises within the range (0.8 Hz, 53 Hz) for the chevron structure (see the higher curve). The result that f_i is higher for the chevron structure than the bookshelf structure was first reported by Blinov et al. (*4*). This is interesting since general opinion is that V-shaped switching is hardly compatible for a chevron structure.

3.3. f_i *dependence on amplitude of applied voltage*

The dependence of f_i on amplitude of the total applied voltage for both bookshelf and chevron structures are shown in Figure 7. The symbols are derived directly from the model and the dotted curves are fitted to the data. The hysteresis inversion frequency f_i increases with increasing voltage in both bookshelf and chevron structures. However the range of f_i is (0.24 Hz, 7.5 Hz) for the bookshelf structure and (1.2 Hz, 8.6 Hz) for chevron structure. Also, f_i for the chevron structure are higher than those for bookshelf structure. The f_i dependence of amplitude

Downloaded At: 15:19 25 January 2011

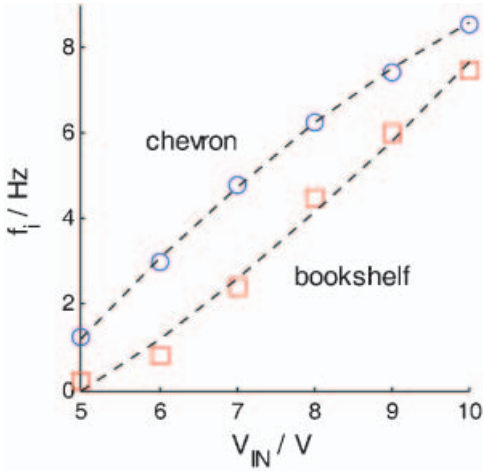

Figure 7. Comparison of the dependence of the hysteresis inversion frequency f_i on the amplitude of total applied voltage for the bookshelf and chevron structures.

of applied voltage is as predicted since it comes from the voltage dependence of the switching time $\tau=\gamma/P_S E$ (*11*) and has been proved by several experimental results (*4, 16*).

3.4. f_i *dependence on spontaneous polarisation*

The dependence of f_i on spontaneous polarisation for both the bookshelf and chevron structures is shown in Figure 8. The figure shows that f_i for the chevron structure is higher than that for the bookshelf structure. Also, f_i shows a maximum as spontaneous polarisation increases in both cases. Take the case of chevron structure for example (see the higher curve), when $P_S<100$ nC, f_i increases as P_S increases. In this sense, high values of P_S are preferable for V-shaped switching as discussed in (*6*). However, as P_S further increases, the curve reaches its maxima and then f_i decreases. This result has been reported by Blinov *et al.* as a simulation result (*4*) and is an important indication of the coincidence of the circuit model with the valuable model. Although the reason for such a tendency is not clear now, it should be taken into account when tailoring new materials for V-shaped switching.

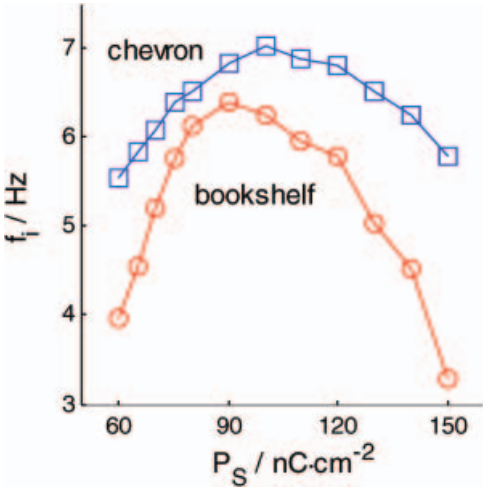

Figure 8. Dependence of the hysteresis inversion frequency on spontaneous polarisation for the chevron and bookshelf structures.

4. Conclusions

An improved equivalent circuit model for V-shaped, thresholdless, hysteresis-free SSFLC cells has been developed. The difference between the improved model and previous circuit models is that the impedance divider induced by the multilayer structure of SSFLC cells is taken into account in the improved model. Also, both polar and non-polar surface-anchoring energy are considered in the improved model. The result that V-shaped switching occurs only at the hysteresis inversion frequency and only when the transmittance is plotted as a function of the total applied voltage is well reproduced by the improved model. Also, the dependence of hysteresis inversion frequency on conductivity of the FLC layer, amplitude of applied voltage and spontaneous polarisation for both bookshelf and chevron structures are simulated; the dependence given by the improved circuit model is in good agreement with the reported theoretical and experimental results. Moreover, since the circuit model is established based on the so-called uniform theory where the director orientation does not vary along the thickness of liquid-crystal cell, it proves that even a homogeneous structure of a SSFLC cell combined with the impedance divider allows an explanation of V-shaped switching. Finally, it should be emphasised that the equivalent circuit model described here is not a unique case; various drive circuits can be conveniently inserted into the model and the model can be extended into general electro-optical devices with the light modulation layer comprising of FLC.

Acknowledgements

This work was supported by the National Natural Science Foundation of China (No. 10174057 and 90201011) and the Key Project of Chinese Ministry of Education (No. 2005-105148).

References

(1) Clark N.A.; Lagerwall S.T. *Appl. Phys. Lett.* **1980**, *36*, 899–901.

Downloaded At: 15:19 25 January 2011

(2) Chandani A.; Cui Y.; Seomun S.S.; Takanishi Y.; Ishikawa K.; Takezoe H.; Fukuda A. *Liq. Cryst.* **1999**, *26*, 151–161, **1999**, *26*, 167–179.
(3) Hayashi N.; Kato T.; Ando T.; Fukuda A.; Kawada S.; Kondoh S. *Phys. Rev. E* **2003** *68*, 011702, 1–9.
(4) Blinov L.M.; Palto S.P.; Podgornov F.V.; Moritake H.; Haase W. *Liq. Cryst.* **2004**, *31*, 61–70.
(5) Vauotič N.; Čopič M. *Phys. Rev. E* **2003**, *68*, 061705, 1–8.
(6) Rudquist P.; Lagerwall J.P.F.; Buivydas M.; Gouda F.; Lagerwall S.T.; Clark N.A.; Maclennan J.E.; Shao R.; Coleman D.A.; Bardon S.; Link D.R.; Natale G.; Glaser M.A.; Walba D.M.; Wang M.D.; Chen X.H. *J. Mater. Chem.* **1999**, *9*, 1257–1262.
(7) Čopič M.; Maclennan J.E.; Clark N.A. *Phys. Rev. E* **2002** *65*, 021708, 1–9.
(8) O' Callaghan M.J. *Phys. Rev. E* **2003**, *67*, 011710, 1–12.
(9) Čopič M.; Maclennan J.E.; Clark N.A. *Phys. Rev. E* **2001** *63*, 031703, 1–5.
(10) Palto S.P.; Geivandov A.R.; Barnik M.I.; Blinov L.M. *Ferroelectrics* **2004**, *310*, 95–109.
(11) Blinov L.M.; Pozhidaev E.P.; Podgornov F.V.; Pikin S.A.; Palto S.P.; Sinha A.; Yasuda A.; Hashimoto S.; Haase W. *Phys. Rev. E* **2002** *66*, 021701, 1–10.
(12) Blinov L.M.; Palto S.P.; Pozhidaev E.P.; Podgornov F.V.; Haase W.; Andreev A.L. *Mol. Crys. Liq. Crys.* **2004**, *410*, 105–115.
(13) Blinov L.M.; Palto S.P.; Pozhidaev E.P.; Bobylev Yu.P.; Shoshin V.M.; Andreev A.L.; Podgornov F.V.; Haase W. *Phys. Rev. E* **2005** *71*, 051715, 1–10.
(14) Blinov L.M.; Pozhidaev E.P.; Podgornov F.V.; Sinha A.; Haase W. *Ferroelectrics* **2002**, *277*, 3–11.
(15) Palto S.P.; Podgornov F.V.; Haase W.; Blinov L.M. *Mol. Crys. Liq. Crys.* **2004**, *410*, 95–104.
(16) Shwu-Yun T.; Lin T.Y.; Huang R.H.; Jin-Jei W.; Shune-Long W. *Phys. Rev. E* **2004**, *70*, 011712, 1–5.
(17) Shwu-Yun T.T.; Huang R.H.; Jin-Jei W.; Shune-Long W. *Jpn. J. Appl. Phys.* **2005**, *44*, 1871–1874.
(18) Moore J.R.; Travis A.R.L. *IEE Proc.-Optoelectron.* **1999**, *146*, 231–237.
(19) Wang M.Y.; Pan W.; Luo B.; Zou X.H.; Zhang W.L. *IET Optoelectron.* (succeeds *IEE Proc.-Optoelectron.*) **2007**, *1*, 16–22.
(20) Lee Y.; Gourlay J.; Hossack W.J.; Underwood I.; Walton A.J. *Microelectron. J.* **2004**, *35*, 193–201.
(21) Wang M.Y.; Pan W.; Luo B.; Zhang W.L.; Zou X.H. *Microelectron. J.* **2007**, *38*, 203–209.
(22) Smith S.; Walton A.J.; Underwood I.; Miremont C.; Vass D.G.; Hossack W.J.; Birch M.; Macartney A.; Nicol R. *SPIE Proc.* **2003**, *5181*, 144–153.
(23) Sako T.; Itoh N.; Sakaigawa A.; Koden M. *Appl. Phys. Lett.* **1997**, *71*, 461–463.
(24) Lagerwall S.T. *Ferroelectric and Antiferroelectric Liquid Crystals*; Wiley-VCH: Weinheim, 1999.
(25) Kiselev A.D.; Chigrinov V.G.; Pozhidaev E.P. *Phys. Rev. E* **2007**, *75*, 061706, 1–15.
(26) Podgornov F.V., Fachbereich Physik, Technische Universität Darmstadt, 37, 2004. http://deposit.ddb.de/cgi-bin/dokserv?idn=971472297.
(27) Jones J.C.; Raynes E.P. *Liq. Crys.* **1992**, *11*, 199–217.

Downloaded At: 15:19 25 January 2011